Advance Access publication on 14 December 2020
doi: 10.1093/comjnl/bxaa150

Real-World Networks Are Not Always Fast Mixing

Yi Qi[1], Wanyue Xu[1], Liwang Zhu[1] and Zhongzhi Zhang[1,2,*]

[1]*Shanghai Key Laboratory of Intelligent Information Processing, School of Computer Science, Fudan University, Shanghai 200433, China*
[2]*Shanghai Engineering Research Institute of Blockchain, Shanghai 200433, China*
**Corresponding author: zhangzz@fudan.edu.cn*

The mixing time of random walks on a graph has found broad applications across both theoretical and practical aspects of computer science, with the application effects depending on the behavior of mixing time. It is extensively believed that real-world networks, especially social networks, are fast mixing with their mixing time at most $O(\log N)$ where N is the number of vertices. However, the behavior of mixing time in the real-life networks has not been examined carefully, and exactly analytical research for mixing time in models mimicking real networks is still lacking. In this paper, we first experimentally evaluate the mixing time of various real-world networks with scale-free small-world properties and show that their mixing time is much higher than anticipated. To better understand the behavior of the mixing time for real-world networks, we then analytically study the mixing time of the Apollonian network, which is simultaneously scale-free and small-world. To this end, we derive the recursive relations for all eigenvalues, especially the second largest eigenvalue modulus of the transition matrix, based on which we deduce a lower bound for the mixing time of the Apollonian network, which approximately scales sublinearly with N. Our results indicate that real-world networks are not always fast mixing, which has potential implications in the design of algorithms related to mixing time.

Keywords: random walk; mixing time; normalized Laplacian; social networks; fast mixing;

Received 16 August 2019; Revised 15 August 2020; Accepted 2 October 2020
Handling editor: Jin-Hee Cho

1. INTRODUCTION

Random walks on a network is a powerful tool in various disciplines, and understanding the behavior of random walks is important for their applications [1, 2]. One of the most important quantities related to random walks is the mixing time [3, 4]. For a discrete-time random walk on a network, the mixing time is defined as the steps the walker needs to jump till it approaches the stationary distribution, regardless of the initial state [5]. Mixing time reflects the global characteristic of a network and has found applications in numerous aspects [4], such as constructing gossip [6] and sampling [7–9] algorithms, and designing security defenses and communication systems [10–13]. Due to the wide range of applications, mixing time has received much recent attention from the scientific community [14–21].

The application effects of mixing time highly rely on the properties of mixing time in the underlying network. It is widely believed that most real-world networks, especially social networks, are fast mixing. That is, for random walks on a graph with N nodes, when the walk length approaches $O(\log N)$, the probability distribution that the walk ends a certain vertex converges to the stationary distribution. Although this property has not been confirmed for real-world networks yet, it has been widely applied in the scenario of building Sybil defenses and anonymous communication systems, with typical examples including SybilLimit [10], SybilGuard [11], SybilInfer [12] and Whanau [22]. All these schemes are based on the assumption that social networks are fast mixing, which has a strong influence on both the performance and security of the systems [13]. Recently, it was reported that for some real-world social networks the mixing time is much higher than anticipated [23]. Thus far, the properties of the mixing time for other real-world networks are still unknown. Particularly, accurate analytical studies on the mixing time of model networks with scale-free [24] small-world [25] properties as observed in realistic networks are still lacking, although it is

important for understanding the behavior of mixing time in actual systems.

In this paper, we study the lower bound of mixing time for various types of real-world networks with different vertex number N, including social networks, metabolic networks, citation networks and so on. By using the link between the mixing time and the eigenvalues of transition matrix, we show that the lower bound for the mixing time of the examined realistic networks is much higher than $O(\log N)$. We then study analytically the mixing time of the Apollonian network with the prominent scale-free small-world properties [26, 27]. For this purpose, we derive the recursion expressions for all the eigenvalues of the transition matrix of the Apollonian network and obtain the second largest eigenvalue modulus characterizing the mixing time. Based on this result, we further evaluate the mixing time of the Apollonian network, which approximately grows as a sublinear function of the number of vertices. Our work implies that fast mixing is not a universal property for real-world networks, especially those with the scale-free and small-world topologies.

2. PRELIMINARIES

In this section, we recall some basic concepts used in this paper, including graph and related matrices, mixing time for random walks on a graph and some related notions and properties about mixing time.

2.1. Graph and Related Matrices

Consider a simple connected undirected unweighted graph (network) $G = (V, E)$, where $V = V(G)$ is the set of vertices and $E = E(G)$ is the set of edges. Let $N = |V|$ denote the order (the number of vertices) and $M = |E|$ denote the size (the number of edges) of graph $G = (V, E)$.

For a graph G, there are several matrices associated with it. The adjacency matrix $\mathbf{A} = (A_{ij})_{N\times N}$ describes the adjacency relation between the N vertices in G, where the entry A_{ij} is defined as follows: $A_{ij} = A_{ji} = 1$, if vertices i and j are connected directly by an edge, $A_{ij} = A_{ji} = 0$ otherwise. Then, the degree of vertex i in G is $d_i = \sum_{j=1}^{N} A_{ij}$. And the diagonal degree matrix of G is defined as $\mathbf{D} = \mathrm{diag}\{d_1, d_2, \ldots, d_n\}$.

From $\mathbf{A}$ and $\mathbf{D}$, we can define the transition matrix $\mathbf{T}$ of G given by $\mathbf{T} = \mathbf{D}^{-1}\mathbf{A}$. Thus, the (i,j)th element of $\mathbf{T}$ is $T(i,j) = A(i,j)/d_i$, which describes the transition probability from vertex i to vertex j in the unbiased random walk taking place on G. In general, the transition matrix $\mathbf{T}$ is asymmetric, with the exception of regular graphs. The normalized adjacency matrix of G is $\mathbf{P} = \mathbf{D}^{-\frac{1}{2}}\mathbf{A}\mathbf{D}^{-\frac{1}{2}}$, which is similar to $\mathbf{T}$ due to the relation $\mathbf{P} = \mathbf{D}^{\frac{1}{2}}\mathbf{T}\mathbf{D}^{-\frac{1}{2}}$. Thus, $\mathbf{T}$ and $\mathbf{P}$ have the same set of eigenvalues. The normalized Laplacian matrix of G is defined by $\mathbf{L} = \mathbf{I} - \mathbf{D}^{-\frac{1}{2}}\mathbf{A}\mathbf{D}^{-\frac{1}{2}}$, where $\mathbf{I}$ is the $N \times N$ identity matrix.

2.2. Mixing Time for Random Walks

For a connected undirected graph $G = (V, E)$ with N vertices and M edges, we can define a discrete-time random walk on it. A simple unbiased random walk $\mu = (\mu_1, \mu_2, \cdots)$ on graph G starting at vertex u is a sequence of stochastic variables μ_k whose domain is the vertex set V such that $\mu_1 = u$ and the probability for $\mu_{k+1} = j$ provided that $\mu_k = i$ is $1/d_i$ for $k = 1, 2, \cdots, N$, where j is a neighbor of vertex i. The random walk μ on a graph G is actually a Markov chain [28], which is characterized by the transition matrix $\mathbf{T}$ of G. Moreover, if graph G is non-bipartite, the random walk μ on G is ergodic, which means that the distribution of μ_t converges to a unique stationary distribution $\pi = (\pi_1, \pi_2, \cdots, \pi_N)$ as $t \to \infty$. It is easy to verify that $\pi_i = \frac{d_i}{2M}$, satisfying $\sum_{i=1}^{N} \pi_i = 1$ and $\pi^\top \mathbf{T} = \pi^\top$.

For different networks, the asymptotic convergence rate is often quite different. In order to measure how quickly a random walk approaches to its limiting distribution, a lot of metrics were proposed [14], among which mixing time is a frequently used one. To quantify the meaning of approaching to the equilibrium distribution, we first introduce a distance measure as follows.

DEFINITION 2.1. *Given two probability distributions D_1 and D_2 on a countable state space S, the variation distance is*

$$||D_1 - D_2|| = \frac{1}{2}\sum_{x\in S} |D_1(x) - D_2(x)|. \tag{1}$$

Let e_x be the xth canonical basis of vector space $\mathbb{R}^N$, with position x being 1 and all other positions being 0. Then, for a random walk starting at vertex x, the probability distribution of the state at different vertices after t steps is $(p_x^t)^\top = e_x^\top \mathbf{T}^t$. And the variation distance $\Delta_x(t)$ between p_x^t and the stationary distribution π is

$$\Delta_x(t) = ||p_x^t - \pi||. \tag{2}$$

Using the notion of variation distance, we can define the mixing time characterized by a parameter ϵ.

DEFINITION 2.2. *Given a threshold $0 < \epsilon < 1$, the mixing time of a vertex x is*

$$T_x(\epsilon) = \min\{t : \Delta_x(t) \le \epsilon\}. \tag{3}$$

And the mixing time of the whole network $G = (V, E)$ with respect to the parameter ϵ is defined as

$$T(\epsilon) = \max_{x\in V} T_x(\epsilon). \tag{4}$$

A network with N vertices is called *fast mixing* if its mixing time is $O(\mathrm{poly}\log N)$ and $O(\mathrm{poly}\log\frac{1}{\epsilon})$ [29]. In this paper, following many previous work [10–12, 23], we strengthen the

definition of mixing time by considering the particular case $\epsilon = \Theta(\frac{1}{n})$, and say a network is fast mixing if its mixing time is not larger than $O(\log N)$.

It is very difficult to compute the mixing time by directly using definition, especially for small ϵ. However, one can bound the mixing time in terms of ϵ and the eigenvalues of transition matrix. Let $\lambda_1, \lambda_2, \lambda_3, \cdots, \lambda_N$ be the N eigenvalues associated with matrix $\mathbf{T}$ of a non-bipartite graph $G = (V, E)$ arranged in a decreasing order, i.e. $1 = \lambda_1 > \lambda_2 \geq \cdots \geq \lambda_N > -1$. Let $\lambda_{2\text{nd}}$ be the second largest eigenvalue modulus (SLEM) of $\mathbf{T}$ defined by $\lambda_{2\text{nd}} = \max\{\lambda_2, |\lambda_N|\}$. The quantity $1 - \lambda_{2\text{nd}}$, often called spectral gap, is closely related to the mixing time $T(\epsilon)$ of graph G, as shown in the following theorem [29].

THEOREM 2.1. *For a non-bipartite graph $G = (V, E)$ with N vertices, the mixing time $T(\epsilon)$ is bounded by*

$$\frac{\lambda_{2nd}}{2(1-\lambda_{2nd})} \log\left(\frac{1}{2\epsilon}\right) \leq T(\epsilon) \leq \frac{\log N + \log(1/\epsilon)}{1-\lambda_{2nd}}. \quad (5)$$

Theorem 2.1 shows that the SLEM $\lambda_{2\text{nd}}$ determines the mixing time of a graph: the smaller $\lambda_{2\text{nd}}$ is, the faster the Markov chain converges.

3. MIXING TIME OF REAL-WORLD NETWORKS

It is a cumbersome task to evaluate accurately the mixing time of random walks in a large network, even if the network structure is known as prior knowledge. In this section, in order to understand the behavior of mixing time in real-world networks, we study the lower bound for the mixing time of various real-life networks, instead of determining the exact values of mixing time. For this purpose, we apply Theorem 2.1 to provide lower bounds of the mixing time for different variation distances.

3.1. Data Sets of Real-World Networks

The datasets we use in our experiment are selected from the Koblenz Network Collection, which are publicly available at the website http://konect.uni-koblenz.de/networks/. The examined datasets include social networks, metabolic networks, citation networks, hyperlink networks and so on. All the networks are both scale free and smallworld. Since we are only concerned with undirected and unweighted networks without multiple edges or self-loops, for each network that is disconnected, we only study the mixing time of its largest connected component. Table 1 summarizes the basic statistics of these real-world networks, including dataset name, vertex number N, edge number M and SLEM $\lambda_{2\text{nd}}$.

3.2. Experiment Results

In order to be able to apply Theorem 2.1, we perform the following preprocessing for each network. First, we eliminate self-loops and isolated vertices. Second, we convert directed or weighted graphs to undirected and unweighted. Last, we extract the largest connected component. After preprocessing, we compute the SLEM of the transition matrix corresponding to the largest connected component of each network, which is shown in the last column of Table 1. We then calculate the lower bound of the mixing time for each network by applying Theorem 2.1. Note that we do not consider the upper bound since it is not relevant to the goal of this paper.

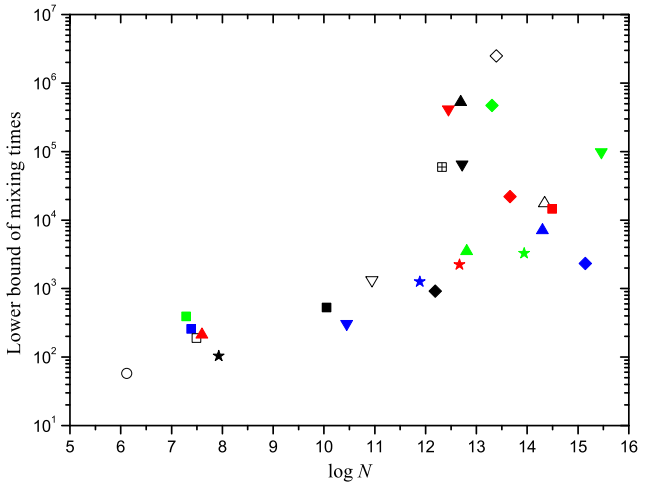

FIGURE 1. Lower bound of the mixing times for various real-world networks corresponding to the variation distance $\epsilon = \frac{1}{N}$. Each symbol corresponds to a network in Table 1: 1. □; 2. ▲; 3. ▽; 4. ♦; 5. ♦; 6. ★; 7. ▲; 8. ▼; 9. ◯; 10. ■; 11. ■; 12. ★; 13. ■; 14. ▼; 15. ▲; 16. ♦; 17. ▼; 18. ▲; 19. ◇; 20, ♦; 21. ■; 22. ★; 23. ⊞; 24. ★; 25. ▼; 26. △.

Figure 1 reports the lower bound of the mixing time corresponding to different variation distance ϵ for different real-world networks. For small-scale networks with the order ranging from 10^3 to 10^5, to achieve a variation distance $\epsilon = 10^{-3}$, the lower bound of the mixing time is larger than 170 for each social network and is in the range between 60 and 400 for metabolic networks. For medium-scale networks with vertex number changing from 10^5 to 10^6, to achieve $\epsilon = 10^{-5}$ the lower bound of the mixing time ranges from 10^4 to 2×10^6 for hyperlink networks. While for large-scale networks with more than 10^7 vertices, the lower bound of the mixing time to achieve $\epsilon = 10^{-7}$ is varying and dependent on network structure. For example, it is about 3796, 8051, 102395 and 19852 for Youtube friendship, Flickr links, LiveJournal links and Skitter, respectively.

As can be seen from Fig. 1, for most of studied real-world networks, they have a larger lower bound for the mixing time than anticipated. In particular, when the variation distance is $\epsilon = \Theta(\frac{1}{N})$, the lower bound of the mixing time is much larger than $O(\log N)$. Since for each network, its actual mixing time is not less than the lower bound obtained by Theorem 2.1, the

TABLE 1. Datasets and related information.

No.	Dataset	N	M	λ_{2nd}	$1/(1-\lambda_{2nd})$
		Social networks			
1	Hamsterster friendships	1788	12476	0.98241332	56.86
2	Hamsterster full	2000	16098	0.98401448	62.56
3	Brightkite	56739	212945	0.99616094	260.48
4	Gowalla	196591	950327	0.99379117	161.06
5	Catster	601213	15661775	0.99998656	74404.76
6	Youtube friendship	1134890	2987624	0.99797217	493.14
7	Flickr links	1624991	15473043	0.99904303	1044.96
8	LiveJournal links	5189808	48687945	0.99992469	13278.45
		Metabolic networks			
9	Caenorhabditis elegans	453	2,025	0.95531072	22.38
10	Protein	1458	1948	0.99166729	120.01
11	Human protein (Stelzl)	1615	3106	0.98718391	78.03
12	Human protein (Vidal)	2783	6007	0.96613589	29.53
		Citation networks			
13	Cora citation	23166	89157	0.99126276	114.45
14	arXiv hep-th	34401	420784	0.98428427	63.63
15	CiteSeer	365154	1721981	0.99828318	582.47
16	US patents	3764117	16511740	0.99690769	323.38
		Hyperlink networks			
17	Stanford	255265	1941926	0.99998576	70224.72
18	Notre Dame	325729	1497134	0.99998858	87565.67
19	Berkeley/Stanford	654782	6581871	0.99999744	390625.00
20	Google	855802	4291352	0.99970457	3384.90
21	Hudong internal links	1962418	14419760	0.99952804	2118.82
		Other networks			
22	WordNet	145145	656230	0.99555639	225.04
23	EU institution	224832	339925	0.99990182	10185.37
24	DBLP Coauthorship	317080	1049866	0.99732109	373.29
25	Amazon (MDS)	334863	925872	0.99990726	10782.83
26	Skitter	1694616	11094209	0.99961165	2575.00

real-world networks used in our experiment do not possess the property of fast mixing.

The above-considered real-world networks are all scale-free and small-world, which are now recognized as two common properties of most real networks [30]. In order to deepen our understanding of the behavior for mixing time of real-life networks, in what follows, we will derive analytically the lower bound of mixing time for the Apollonian network with the striking scale-free small-world features [27]. We will show that the Apollonian network is also not fast mixing, since the lower bound of its mixing time scales sublinearly with the vertex number.

4. MIXING TIME OF THE APOLLONIAN NETWORK

In the section, we study analytically the mixing time for random walks on the Apollonian network with the remarkable scale-free and small-world characteristics.

4.1. Network Construction and Properties

The Apollonian network is generated by an iterative manner [27]. Let $\mathcal{A}(n), n \geq 1$, denote the Apollonian network after n iterations. For $n = 1, \mathcal{A}(1)$ is a tetrahedron consisting of four faces or triangles. For $n \geq 2, \mathcal{A}(n)$ is obtained from $\mathcal{A}(n-1)$ by executing the following operation: for each existing triangle in $\mathcal{A}(n-1)$ that was created at iteration $n-1$, a new vertex is generated and connected to all the three vertices of this triangle. Let N_n and E_n denote the order and the size of the Apollonian network $\mathcal{A}(n)$, respectively. Then, for all $n \geq 1, N_n = 2 \cdot 3^{n-1} + 2$ and $E_n = 2 \cdot 3^n$. Figure 2 shows the initial structure of $\mathcal{A}(1)$ and an illustration construction of the Apollonian network.

The Apollonian network exhibits the representative characteristics of real-life networks in nature and society. First, it is scale-free with its vertex degree obeying a power-law distribution $P(k) \sim k^{-(1+\frac{\ln 3}{\ln 2})}$ [27]. Second, it is small-world with its diameter D_n growing logarithmically with N_n [31]. Finally,

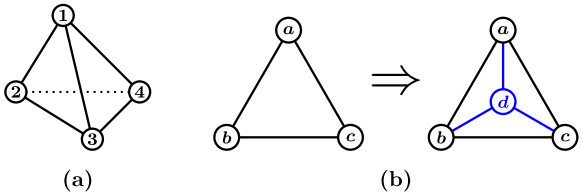

FIGURE 2. (a) The initial construction of Apollonian network $\mathcal{A}(1)$. (b) Iterative construction way of the Apollonian network.

it is highly clustered with its average clustering coefficient approaching to a large constant 0.8284. Thus, the Apollonian network is a good model for real-world networks, the properties of which are much studied [32–36].

4.2. All Eigenvalues of Related Matrices

According to Theorem 2.1, it is an easy task to bound the mixing time of a graph if we know the full eigenvalues of its transition matrix. However, for a general huge graph, it is a challenge to determine the eigenvalues of its transition matrix, due to the limit of time and memory. For the particular case of the Apollonian network, we can find all the eigenvalues of related matrix by using the decimation technique [37] and its particular structure. In what follows, we will derive analytically all the eigenvalues and their corresponding multiplicities of the Apollonian network, based on which we will further evaluate the mixing time of the network.

Let $\mathbf{T}_n$ and $\mathbf{P}_n$ denote the transition matrix and normalized adjacency matrix of the Apollonian network $\mathcal{A}(n)$, respectively. Let Ψ_n be the set of eigenvalues of $\mathbf{T}_n$ or $\mathbf{P}_n$:

$$\Psi_n = \left\{\lambda_1^{(n)}, \lambda_2^{(n)}, \cdots, \lambda_{N_n}^{(n)}\right\}, \tag{6}$$

with the elements obeying relation $1 = \lambda_1^{(n)} > \lambda_2^{(n)} \geq \cdots \geq \lambda_{N_n}^{(n)} > -1$. Note that Ψ_n is a multiset, in which the distinctness of the elements is neglected.

LEMMA 4.1. *Let λ be a nonzero eigenvalue of $\mathbf{P}_n$. Define the function $R(x)$ of a real variable x as $R(x) = \frac{6x^2-1}{3x+2}$. Then, $R(\lambda)$ is an eigenvalue of $\mathbf{P}_{n-1}$ with the same multiplicity as λ.*

Proof. Let V_n be set of vertices in $\mathcal{A}(n)$. Then, V_n can be divided into two disjoint sets: V_{n-1} and V'_n, where V_{n-1} contains all the vertices inherited from $\mathcal{A}(n-1)$ and V'_n includes all the newly vertices generated at iteration n, i.e. $V'_n = V_n \setminus V_{n-1}$. For a vertex $i \in V_n$, let $N_n(i) = \{j|A_n(i,j) = 1\}$ denote the set of its neighbors. Then, $N_n(i)$ is the union of two disjoint sets $N_n^1(i)$ and $N_n^2(i)$, where $N_n^1(i) = N_n(i) \cap V_{n-1}$ and $N_n^2(i) = N_n(i) \cap V'_n$.

Let $\mathbf{x} = (x_1, x_2, \cdots, x_{N_n})^\top$ be an eigenvector corresponding to the eigenvalue λ of $\mathbf{P}_n$. Then,

$$\mathbf{P}_n\mathbf{x} = \lambda\mathbf{x}, \tag{7}$$

where the row corresponding to vertex i can be written as

$$\sum_{j\in N_n(i)} P_n(i,j)x_j = \lambda x_i. \tag{8}$$

If $i \in V_{n-1}$, let $B(n,i)$ denote the sum on the left hand side of (8). Then, $B(n,i)$ can be expressed as

$$B(n,i) = B_1(n,i) + B_2(n,i), \tag{9}$$

where $B_1(n,i) = \sum_{j\in N_n^1(i)} P_n(i,j)x_j$ and $B_2(n,i) = \sum_{j\in N_n^2(i)} P_n(i,j)x_j$.

By construction, $B_2(n,i)$ can be evaluated as

$$B_2(n,i) = \sum_{j\in N_n^2(i)} \frac{x_j}{\sqrt{k_i(n)}\sqrt{k_j(n)}} = \sum_{j\in N_n^2(i)} \frac{x_j}{\sqrt{k_i(n)}\sqrt{3}}. \tag{10}$$

For any vertex $j \in N_n^2(i)$, we have

$$x_j = \frac{1}{\lambda}\sum_{k\in N_n(j)} P_n(j,k)x_k = \frac{1}{\lambda}\sum_{k\in N_n(j)} \frac{x_k}{\sqrt{k_k(n)}\sqrt{3}}. \tag{11}$$

Inserting (11) into (10) yields

$$\begin{aligned} B_2(n,i) &= \frac{1}{3\lambda}\sum_{j\in N_n^2(i),k\in N_n(j)} \frac{x_k}{\sqrt{k_i(n)}\sqrt{k_k(n)}} \\ &= \frac{1}{3\lambda}\left(\sum_{j\in N_n^2(i),k\in N_n(j),k\neq i} \frac{x_k}{\sqrt{k_i(n)}\sqrt{k_k(n)}} + \frac{|N_n^2(i)|x_i}{k_i(n)}\right) \\ &= \frac{1}{3\lambda}\left(2B_1(n,i) + \frac{x_i}{2}\right). \end{aligned} \tag{12}$$

Combining (12) and (9), we obtain the following relation:

$$B(n,i) = \frac{3\lambda+2}{3\lambda}B_1(n,i) + \frac{x_i}{6\lambda} = \lambda x_i, \tag{13}$$

which can be recast as

$$2B_1(n,i) = \frac{6\lambda^2-1}{3\lambda+2}x_i. \tag{14}$$

On the other hand, by construction of $\mathcal{A}(n)$, we have

$$2B_1(n,i) = B(n-1,i), \tag{15}$$

which, together with (14), shows that $R(\lambda) = \frac{6\lambda^2-1}{3\lambda+2}$ is an eigenvalue of P_{n-1}, with $\mathbf{x}' = (x_i)_{i\in V_{n-1}}^\top$ being one of its corresponding eigenvectors.

For any vertex $j \in V'_n$, according to (7), its entry x_j of vector $\mathbf{x}$ satisfies

$$x_j = \frac{1}{\lambda} \sum_{k \in N_n(j)} P_n(j,k) x_k. \tag{16}$$

Note that for any vertex $j \in V'_n$ and any element $k \in N_n(j)$, we have $k \in V_{n-1}$. Thus, $\mathbf{x}$ is totally determined by $\mathbf{x}'$ as given in (16). Let $m_n(\lambda)$ be the multiplicity of an eigenvalue λ for matrix $\mathbf{P}_n$. Then, $m_{n-1}(R(\lambda)) \geq m_n(\lambda)$. We now prove that only the equality holds. Suppose that $m_{n-1}(R(\lambda)) > m_n(\lambda)$. This indicates that there should exist an extra eigenvector $\mathbf{x}'$ associated to $R(\lambda)$ without a corresponding eigenvector $\mathbf{x}$ in $\mathbf{P}_n$. But (16) provides $\mathbf{x}$ with an associated eigenvector of $\mathbf{P}_n$, which contradicts our assumption. Therefore, $m_{n-1}(R(\lambda)) = m_n(\lambda)$. ■

We define two functions $h_1(x)$ and $h_2(x)$ for real variable x:

$$h_1(x) = \frac{1}{12}\left(3x - \sqrt{9x^2 + 48x + 24}\right) \tag{17}$$

and

$$h_2(x) = \frac{1}{12}\left(3x + \sqrt{9x^2 + 48x + 24}\right). \tag{18}$$

Then, we have the following lemma.

LEMMA 4.2. *Let λ be any eigenvalue of $\mathbf{P}_{n-1}$ such that $\lambda \neq -\frac{1}{2}$, then $h_1(\lambda)$ and $h_2(\lambda)$ are eigenvalues of $\mathbf{P}_n$, besides $m_n(h_1(\lambda)) = m_n(h_2(\lambda)) = m_{n-1}(\lambda)$.*

Proof. This lemma is a direct consequence of Lemma 4.1. ■

Lemmas 4.1 and 4.2 show that any non-zero eigenvalue of $\mathbf{P}_n$ can be obtained from that of $\mathbf{P}_{n-1}$. Moreover, each eigenvalue $\lambda \neq -\frac{1}{2}$ of $\mathbf{P}_{n-1}$ gives rise two eigenvalues of $\mathbf{P}_n$ given by $h_1(\lambda)$ and $h_2(\lambda)$. Thus, what is left is to determine the multiplicity of the zero eigenvalue of $\mathbf{P}_n$.

LEMMA 4.3. *For $n > 2$, the multiplicity of eigenvalue 0 of $\mathbf{P}_n$ is $m_n(0) = 2 \cdot 3^{n-2} - 1$.*

Proof. Note that for any $n \geq 1$, the multiplicity of eigenvalue 1 of $\mathbf{P}_n$ is 1, i.e. $m_n(1) = 1$. Because $h_1(1) = -\frac{1}{2}$ and $h_2(-\frac{1}{2}) = 0$, we have $m_n(-\frac{1}{2}) = 1$ for any $n \geq 2$. Then, among the $2N_{n-1}$ eigenvalues of $\mathbf{P}_n$ ($n > 2$), which are generated from those of $\mathbf{P}_{n-1}$ by functions $h_1(x)$ and $h_2(x)$, only one is 0. Thus, for $n > 2$, the multiplicity of eigenvalue 0 for $\mathbf{P}_n$ is $m_n(0) = 1 + N_n - 2N_{n-1} = 2 \cdot 3^{n-2} - 1$. ■

DEFINITION 4.4. *Let $U = \{u_1, u_2, \cdots, u_k\}$ denote a finite multiset of real number. Define the multiset $R^{-1}(U)$ to be*

$$R^{-1}(U) = \{h_1(u_1), h_1(u_2), \cdots, h_1(u_k), h_2(u_1), h_2(u_2), \cdots, h_2(u_k)\}. \tag{19}$$

By using Lemmas 4.1, 4.2, and 4.3, the spectrum of $\mathbf{P}_n$ can be fully determined.

THEOREM 4.1. *For $n \geq 2$, the eigenvalue set Ψ_n of matrix $\mathbf{P}_n$ can be classified into two subsets Ψ_n^1 and Ψ_n^2, satisfying $\Psi_n = \Psi_n^1 \cup \Psi_n^2$, where $\Psi_n^1 = R^{-1}(\Psi_{n-1})$ and Ψ_n^2 contains only eigenvalue 0 with multiplicity $N_n - 2N_{n-1} = 2 \cdot 3^{n-2} - 2$.*

For the initial network $\mathcal{A}(1)$, the set of eigenvalues for matrix $\mathbf{P}_1$ is $\Psi_1 = \{-\frac{1}{3}, -\frac{1}{3}, -\frac{1}{3}, 1\}$. By iteratively applying Theorem 4.1, we obtain all the eigenvalues of matrix $\mathbf{P}_n$ for $n \geq 2$.

Let $\mathbf{L}_n$ denote the normalized Laplacian matrix of the Apollonian network $\mathcal{A}(n)$. Since there is a one-to-one correspondence relation for the eigenvalues between the transition matrix $\mathbf{P}_n$ and the normalized Laplacian matrix $\mathbf{L}_n$, we can easily obtain the eigenvalues for $\mathbf{L}_n$. Let the multiset Φ_n represent the set of eigenvalues of $\mathbf{L}_n$ defined as

$$\Phi_n = \left\{\eta_1^{(n)}, \eta_2^{(n)}, \cdots, \eta_{N_n}^{(n)}\right\}, \tag{20}$$

with the eigenvalues obeying $0 = \eta_1^{(n)} < \eta_2^{(n)} \leq \cdots \leq \eta_{N_n}^{(n)} < 2$. In order to conveniently express the eigenvalues of $\mathbf{L}_n$, we define two functions $r_1(x)$ and $r_2(x)$ for real variable x as follows:

$$r_1(x) = \frac{1}{12}\left(3x + 9 - \sqrt{9x^2 - 66x + 81}\right) \tag{21}$$

and

$$r_2(x) = \frac{1}{12}\left(3x + 9 + \sqrt{9x^2 - 66x + 81}\right). \tag{22}$$

Based on the relation governing eigenvalues for matrices $\mathbf{L}_n$ and $\mathbf{P}_n$, we can find all the eigenvalues for $\mathbf{L}_n$.

COROLLARY 4.1. For $n \geq 2$, the eigenvalue set Φ_n of matrix $\mathbf{L}_n$ can be classified into two subsets Φ_n^1 and Φ_n^2, satisfying $\Phi_n = \Phi_n^1 \cup \Phi_n^2$, where Φ_n^1 can be expressed in the following form

$$\Phi_n^1 = \left\{r_1(\eta_1^{(n-1)}), r_1(\eta_2^{(n-1)}), \cdots, r_1(\eta_{N_{n-1}}^{(n-1)}), r_2(\eta_1^{(n-1)}), r_2(\eta_2^{(n-1)}), \cdots, r_2(\eta_{N_{n-1}}^{(n-1)})\right\}, \tag{23}$$

and Φ_n^2 contains only eigenvalue 1 with multiplicity $N_n - 2N_{n-1} = 2 \cdot 3^{n-2} - 2$.

4.3. Second Smallest Eigenvalue for Normalized Laplacian Matrix

For a connected graph, its second smallest eigenvalue of the normalized Laplacian matrix is relevant to diverse dynamical processes in the graph, for example, the mixing time of random walks. Next we evaluate the second smallest eigenvalue of the normalized Laplacian matrix $\mathbf{L}_n$ for the Apollonian network.

THEOREM 4.2. *For the Apollonian network $\mathcal{A}(n)$, the second smallest eigenvalue $\eta_2^{(n)}$ of matrix $\mathbf{L}_n$ can be bounded by*

$$\eta_2^{(n)} = \Theta\left((5/9)^n\right), \tag{24}$$

when $n \to \infty$.

Proof. It is obvious that for $x \in [0,2]$, function $r_1(x)$ (or $r_2(x)$) is a monotonically decreasing (or increasing) function. Moreover, for a given $x, r_1(x) \geq r_2(x)$. According to the Corollary 4.1, for any $n > 1$, the second smallest eigenvalue $\eta_2^{(n)}$ satisfies the following recursion relation:

$$\eta_2^{(n)} = r_1(\eta_2^{(n-1)}). \tag{25}$$

Thus, we have

$$\eta_2^{(n)} - \eta_2^{(n-1)} = \frac{2\eta_2^{(n-1)}(3\eta_2^{(n-1)} - 4)}{9 - 9\eta_2^{(n-1)} + \sqrt{9\left(\eta_2^{(n-1)}\right)^2 - 66\eta_2^{(n-1)} + 81}}. \tag{26}$$

Note that $\eta_2^{(n-1)} < 1$ for any $n > 2$. On the other hand, from (26) we have $\eta_2^{(n)} < \eta_2^{(n-1)}$, indicating that the sequence $\{\eta_2^{(n)}\}_{n=1}^{\infty}$ is decreasing and bounded. Thus, the limit $\lim_{n\to\infty} \eta_2^{(n)}$ exists. Let $\lim_{n\to\infty} \eta_2^{(n)} = \eta$ and substitute it into (25) yields

$$\lim_{n\to\infty} \eta_2^{(n)} = \eta = 0. \tag{27}$$

According to (25), we have

$$\eta_2^{(n)} = \frac{5\eta_2^{(n-1)}}{9 + o(1)}, \tag{28}$$

which indicates that the sequence $\{\eta_2^{(n)}\}_{n=1}^{\infty}$ tends to decay exponentially as $\eta_2^{(n)} = u\left(\frac{5}{9}\right)^n$ for $n \to \infty$. In fact,

$$\lim_{n\to\infty} \frac{u\left(\frac{5}{9}\right)^n}{\frac{1}{12}\left(3u(\frac{5}{9})^{n-1} + 9 - \sqrt{9u^2(\frac{5}{9})^{2n-2} - 66u(\frac{5}{9})^{n-1} + 81}\right)} = 1. \tag{29}$$

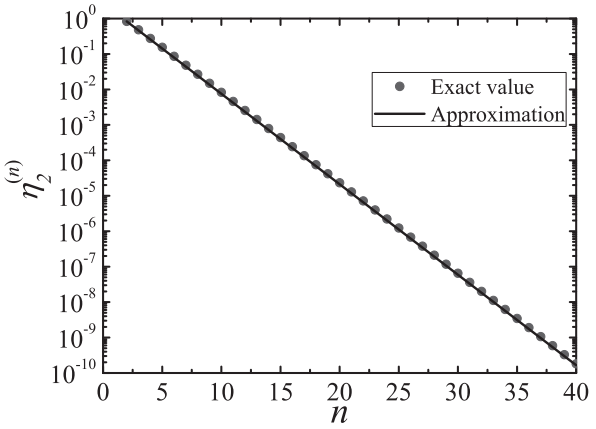

FIGURE 3. The second smallest eigenvalue $\eta_2^{(n)}$ of $\mathbf{L}_n$ for various n.

Thus, for sufficiently large n, the second smallest eigenvalue $\eta_2^{(n)}$ of $\mathbf{L}_n$ can be bounded by $\eta_2^{(n)} = \Theta\left((5/9)^n\right)$. ■

Ignoring the higher order infinitesimal in (28), we obtain a recursion relation of $\eta_2^{(n)}$ as $\eta_2^{(n)} \approx \frac{5}{9}\eta_2^{(n-1)}$. Considering the fact that $\eta_2^{(2)} = \frac{5}{6}$, we obtain an approximation value $\eta_2^{(n)}$ as $n \to \infty$:

$$\eta_2^{(n)} = \frac{5}{6}\left(\frac{5}{9}\right)^{n-2}. \tag{30}$$

In Fig. 3, we shows the accurate and approximative results for the second smallest eigenvalues $\eta_2^{(2)}$, which are generated by (25) and (30), respectively. It is clear that the results yielded by (25) and (30) agree with each other, with their difference being intangible.

4.4. Mixing Time

We are now in position to apply the obtained eigenvalues to determine the mixing time for the Apollonian network $\mathcal{A}(n)$, denoted by $T_n(\epsilon)$.

THEOREM 4.3. *For large n, the mixing time $T_n(\epsilon)$ of the Apollonian network $\mathcal{A}(n)$ can be bounded by*

$$T_n(\epsilon) = \Omega\left((N_n)^{2-\log_3 5}\right). \tag{31}$$

For $\epsilon = \Theta(1/N_n)$, the bound of the mixing time is

$$T_n(\epsilon) = \Theta\left((N_n)^{2-\log_3 5}\log N_n\right). \tag{32}$$

Proof. Functions $h_1(x)$ and $h_2(x)$ are monotonically decreasing and increasing functions on the domain $x \in (-1,1)$, respectively. Thus, for the smallest eigenvalue in set Ψ_n, we have $\lambda_{N_n}^{(n)} = \min\{h_1(\lambda_{N_1}^{(n-1)}), h_2(\lambda_{N_{n-1}}^{(n-1)})\} \geq -\frac{1}{2}$, implying

that $|\lambda_{N_n}^{(n)}| \leq \frac{1}{2}$. While for $\lambda_2^{(n)}$, we have $\lim_{n\to\infty} \lambda_2^{(n)} = 1 - \lim_{n\to\infty} \eta_2^{(n)} = 1$. Thus, the SLEM $\lambda_{2\text{nd}}^{(n)}$ of $\mathcal{A}(n)$ obeys $\lambda_{2\text{nd}}^{(n)} = \max\{\lambda_2^{(n)}, |\lambda_{N_n}^{(n)}|\} = \lambda_2^{(n)}$. For large n, the SLEM $\lambda_{2\text{nd}}^{(n)}$ can be expressed as

$$\lambda_{2\text{nd}}^{(n)} = 1 - \eta_2^{(n)} = 1 - \Theta\left((5/9)^n\right). \tag{33}$$

Considering $N_n = 2 \cdot 3^{n-1} + 2$, one obtains

$$n = \log_3(N_n - 2) + 1 - \log_3 2. \tag{34}$$

Plugging (34) into (33) leads to

$$\lambda_{2\text{nd}}^{(n)} = 1 - \Theta\left((N_n)^{2-\log_3 5}\right). \tag{35}$$

By Theorem 2.1, the mixing time of $\mathcal{A}(n)$ is bounded by

$$T_n(\epsilon) = \Omega\left((N_n)^{2-\log_3 5}\right). \tag{36}$$

For $\epsilon = \Theta(1/N_n)$, we have

$$T_n(\epsilon) = \Theta\left((N_n)^{2-\log_3 5} \log N_n\right). \tag{37}$$

This completes the proof. ■

Theorem 4.3 provides a lower bound $\Omega\left((N_n)^{2-\log_3 5}\right)$ of the mixing time for the Apollonian network $\mathcal{A}(n)$, which increases sublinearly with the network order N_n. This is much less than the bound of mixing time for regular rings that grows as the square of their order [38]. Thus, although the Apollonian network has a smaller mixing time than that of regular rings, it does not possess the fast mixing property.

In Fig. 4, we display the lower bound for the mixing time $T_n(\epsilon)$ of the Apollonian network $\mathcal{A}(n)$ given by (5) and (33) for different n and ϵ. From Fig. 4, we can observe that each curve in double-logarithmic scale is nearly a straight line, especially in the region of large N_n, which means that the lower bound of mixing time $T_n(\epsilon)$ in the Apollonian network $\mathcal{A}(n)$ exhibits approximately a power-law function of the network order N_n.

Note that for most real-world scale-free networks, the degree distribution $P(k)$ of their vertices takes a power law form $k^{-\gamma}$ with the power exponent γ lies between 2 and 3 [30]. Although we only study analytically the mixing time of the Apollonian network with $\gamma = 1 + \ln 2/\ln 3$, it is not difficult to construct other deterministic scale-free networks with varying $\gamma \in [2, 3]$, for which the lower bound of mixing time also scales sublinearly with the number of vertices.

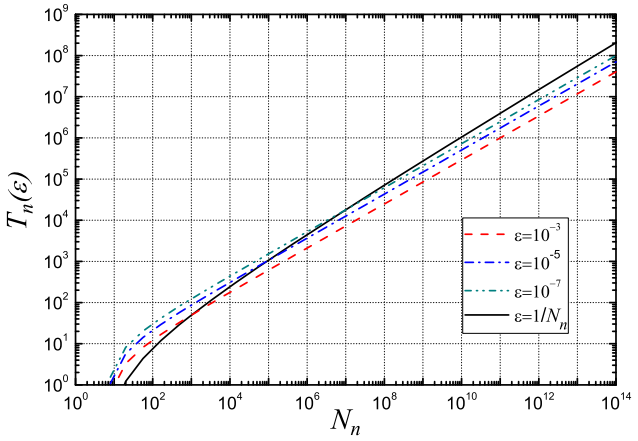

FIGURE 4. The lower bound for the mixing time $T_n(\epsilon)$ of the Apollonian network $\mathcal{A}(n)$ for various n and ϵ.

5. CONCLUSION

As an important parameter of random walks on a network, the mixing time has found broad applications, with its application effects heavily depending on its behavior. It is believed that real-world networks, especially social networks, are fast mixing, with their mixing time scaling at most $O(\log N)$. However, the behavior of mixing time for real-world networks is not well understood. Furthermore, many real-world networks are scale-free and small-world, thus far there have been no rigourous results about mixing time for model networks with these two common properties of realistic systems. In this paper, we experimentally studied the mixing time of various real-world scale-free small-world networks, such as social networks, metabolic networks and citation networks. We evaluated the lower bounds of mixing time for many real-world networks, by using their link with SLEM. Our results show that the observed lower bounds are larger than previous works anticipated, implying that these examined networks are not fast mixing.

In order to better understand the mixing time in scale-free small-world networks, we further presented an analytical research for mixing time of the Apollonian network. By using the decimation technique, we fully characterized the eigenvalues and their corresponding multiplicities for the transition matrix of the Apollonian network. We also derived analytically the SLEM of the transition matrix and obtained the asymptotic behavior of the mixing time of the Apollonian network, which is approximately a power-law function of the number of vertices, with the power exponent slightly smaller than 1. Therefore, the Apollonian network is not fast mixing. Our work deepens the understanding of mixing time in real-world networks and provides useful insights into future applications of the mixing time.

Funding

This work was supported by the National Natural Science Foundation of China (Nos. 61872093, 61803248, U20B2051, and U19A2066)

REFERENCES

[1] Condamin, S., Benichou, O., Tejedor, V., Voituriez, R. and Klafter, J. (2007) First-passage times in complex scale-invariant media. *Nature*, 450, 77–80.

[2] Gallos, L.K., Song, C., Havlin, S. and Makse, H.A. (2007) Scaling theory of transport in complex biological networks. *Proc. Natl. Acad. Sci. U.S.A.*, 104, 7746–7751.

[3] Montenegro, R. and Tetali, P. (2006) Mathematical aspects of mixing times in Markov chains. *Found. Trends Theor. Comput. Sci.*, 1, 237–354.

[4] Levin, D.A., Peres, Y. and Wilmer, E.L. (2009) *Markov Chains and Mixing Times*. American Mathematical Society, Providence, RI.

[5] Buot, M. (2006) Probability and computing: randomized algorithms and probabilistic analysis. *J. Am. Stat. Assoc.*, 101, 395–396.

[6] Boyd, S., Ghosh, A., Prabhakar, B. and Shah, D. (2006) Randomized gossip algorithms. *IEEE Trans. Inf. Theory*, 52, 2508–2530.

[7] Wei, W., Erenrich, J. and Selman, B. (2004) Towards efficient sampling: exploiting random walk strategies. In *Proc. 18th AAAI Conf. Artificial Intelligence*, July, pp. 670–676. AAAI, San Jose, California, USA.

[8] Chiericetti, F., Dasgupta, A., Kumar, R., Lattanzi, S. and Sarlós, T. (2016) On sampling nodes in a network. In *Proc. 25th Int. Conf. World Wide Web*, April 11–15, pp. 471–481. International World Wide Web Conferences Steering Committee, Montreal, Canada.

[9] Zhao, J., Wang, P., Lui, J.C., Towsley, D. and Guan, X. (2019) Sampling online social networks by random walk with indirect jumps. *Data Min. Knowl. Disc.*, 33, 24–57.

[10] Yu, H., Gibbons, P.B., Kaminsky, M. and Xiao, F. (2008) Sybillimit: a near-optimal social network defense against sybil attacks. In *IEEE Symposium on Security and Privacy*, May 18–21, pp. 3–17. IEEE, Oakland, California, USA.

[11] Yu, H., Kaminsky, M., Gibbons, P.B. and Flaxman, A.D. (2008) Sybilguard: defending against sybil attacks via social networks. *IEEE/ACM Trans. Netw.*, 16, 576–589.

[12] Danezis, G. and Mittal, P. (2009) Sybilinfer: detecting sybil nodes using social networks. In *Proc. 16th Network and Distributed System Security Conf.*, February, pp. 1–15. IEEE, San Diego, California, USA.

[13] Yu, H. (2011) Sybil defenses via social networks: a tutorial and survey. *ACM SIGACT News*, 42, 80–101.

[14] Boyd, S., Diaconis, P. and Xiao, L. (2004) Fastest mixing Markov chain on a graph. *SIAM Rev.*, 46, 667–689.

[15] Addario-Berry, L. and Lei, T. (2012) The mixing time of the Newman–Watts small world. In *Proc. Twenty-Third Annual ACM–SIAM Symposium on Discrete Algorithms*, January, pp. 1661–1668. SIAM ACM, Kyoto, Japan.

[16] Benjamini, I., Kozma, G. and Wormald, N. (2014) The mixing time of the giant component of a random graph. *Random Struct. Algor.*, 45, 383–407.

[17] Hsu, D.J., Kontorovich, A. and Szepesvári, C. (2015) Mixing time estimation in reversible Markov chains from a single sample path. In *Proc. 28th Int. Conf. Neural Information Processing Systems*, pp. 1459–1467. Palais des Congres de Montreal, Montreal, Canada.

[18] Talvitie, T., Niinimäki, T. and Koivisto, M. (2017) The mixing of Markov chains on linear extensions in practice. In *Proc. 26th Int. Joint Conf. Artificial Intelligence*, February 19–25, pp. 524–530. AAAI, San Francisco, California USA.

[19] Agostini, M., Bressan, M. and Haddadan, S. (2019) Mixing time bounds for graphlet random walks. *Inform. Process. Lett.*, 152, 105851.

[20] Choi, M.C. and Huang, L.-J. (2020) On hitting time, mixing time and geometric interpretations of metropolis–hastings reversiblizations. *J. Theor. Probab.*, 33, 1144–1163.

[21] Caraceni, A. and Stauffer, A. (2020) Polynomial mixing time of edge flips on quadrangulations. *Probab. Theory Relat. Fields*, 176, 35–76.

[22] Chris Lesniewskilaas, M.F.K. (2012) Whanau: asybil-proof distributed hashtable. In *Proc. 9th Usenix Conf. Networked Systems Design and Implementation*, April, pp. 111–126. USENIX Association, San Jose, California, USA.

[23] Mohaisen, A., Yun, A. and Kim, Y. (2010) Measuring the mixing time of social graphs. In *Proc. 10th ACM SIGCOMM Conf. Internet Measurement*, pp. 383–389. ACM, Melbourne, Australia.

[24] Barabási, A.-L. and Albert, R. (1999) Emergence of scaling in random networks. *Science*, 286, 509–512.

[25] Watts, D.J. and Strogatz, S.H. (1998) Collective dynamics of 'small-world' networks. *Nature*, 393, 440–442.

[26] Andrade, J.S.Jr., Herrmann, H.J., Andrade, R.F. and Da Silva, L.R. (2005) Apollonian networks: simultaneously scale-free, small world, Euclidean, space filling, and with matching graphs. *Phys. Rev. Lett.*, 94, 018702.

[27] Doye, J.P. and Massen, C.P. (2005) Self-similar disk packings as model spatial scale-free networks. *Phys. Rev. E*, 71, 016128.

[28] Kemeny, J.G. and Snell, J.L. (1983) *Finite Markov Chains*. Springer-Verlag, New York, Berlin, Heidelberg, Tokyo.

[29] Alistair, S. (1992) Improved bounds for mixing rates of Markov chains and multicommodity flow. *Combin. Probab. Comput.*, 1, 351–370.

[30] Newman, M.E.J. (2003) The structure and function of complex networks. *SIAM Rev.*, 45, 167–256.

[31] Zhang, Z., Rong, L. and Zhou, S. (2006) Evolving Apollonian networks with small-world scale-free topologies. *Phys. Rev. E*, 74, 046105.

[32] Zhang, Z., Wu, B. and Comellas, F. (2014) The number of spanning trees in Apollonian networks. *Discrete Appl. Math.*, 169, 206–213.

[33] Liao, Y., Hou, Y. and Shen, X. (2014) Tutte polynomial of the Apollonian network. *J. Stat. Mech. Theory Exp.*, 2014, P10043.

[34] Zhang, P. and Mahmoud, H. (2016) The degree profile and weight in Apollonian networks and k-trees. *Adv. Appl. Prob.*, 48, 163–175.

[35] Jin, Y., Li, H. and Zhang, Z. (2017) Maximum matchings and minimum dominating sets in Apollonian networks and extended Tower of Hanoi graphs. *Theoret. Comput. Sci.*, 703, 37–54.

[36] Sheng, Y. and Zhang, Z. (2019) Low-mean hitting time for random walks on heterogeneous networks. *IEEE Trans. Inf. Theory*, 65, 6898–6910.

[37] Teplyaev, A. (1998) Spectral analysis on infinite Sierpiński gaskets. *J. Funct. Anal.*, 159, 537–567.

[38] Gerencser, B. (2011) Markov chain mixing time on cycles. *Stoch. Process. Appl.*, 121, 2553–2570.